

We are IntechOpen, the world's leading publisher of Open Access books Built by scientists, for scientists

6,900

Open access books available

186,000

International authors and editors

200M

Downloads

Our authors are among the

154

Countries delivered to

TOP 1%

most cited scientists

12.2%

Contributors from top 500 universities



WEB OF SCIENCE™

Selection of our books indexed in the Book Citation Index
in Web of Science™ Core Collection (BKCI)

Interested in publishing with us?
Contact book.department@intechopen.com

Numbers displayed above are based on latest data collected.
For more information visit www.intechopen.com



New Technology: Femtosecond Laser May be Used for Future Acupuncture Therapy

Yutaka Takaoka, Mika Ohta, Aki Sugano,
Akihiko Ito and Yoichiro Hosokawa

Additional information is available at the end of the chapter

<http://dx.doi.org/10.5772/54315>

1. Introduction

Acupuncture therapy is utilized to cure many diseases and to maintain health. We have been studying the molecular mechanism of acupuncture and obtained its molecular evidence [1-4]. The World Health Organization has listed more than 40 indications for acupuncture [5], and the National Institutes of Health (NIH) has accepted the validity of acupuncture treatment [6,7]. One of the popular uses of acupuncture treatment is to treat muscle exhaustion, including stiff shoulders. Major acupuncture techniques involve penetration of the skin by thin, solid metallic needles, which are manipulated manually or are stimulated electrically. The efficacy of such muscle therapy is attributed to the overproliferation of muscle cells induced by the damage of muscle in response to the needle penetration. We recently reported that myostatin gene expression is suppressed by electroacupuncture (EA) [1].

However, we cannot exclude the possibility of infection for use of acupuncture, and thus a noncontact method without using needles is needed. Furthermore the laser treatment has a potential for high-throughput therapy. When an intense femtosecond laser is focused on biological tissue, laser ablation is induced at the laser focal spot. Since the main component of the tissue is water, the initiation process occurs with the mutual interaction between water molecules and the femtosecond laser pulse. In comparison with picosecond or nanosecond laser irradiation, the excitation energy of water molecules after the femtosecond laser irradiation is effectively converted to energy to generate shock and stress waves [8,9]. This means simultaneously that heat generation at the laser focal spot is suppressed because of effective energy conversion to these kinetic waves [10]. As a result, when the femtosecond laser is focused on the tissue with suitable irradiation conditions, we can expect that the tissue will be

stimulated mechanically, rather than thermally, by the photomechanical ablation. In previous studies we realized several single-cell manipulation techniques using shock and stress waves under a microscope, including noncontact detachment of an animal cell from its cultured substrate [11,12], control of cell multiplication [13], and estimation of intercellular adhesion strength [14,15]. These techniques can be utilized not only for single cells but also for tissues and organs of living animal. As one of the promising approach, our attention is directed to acupuncture treatment.

In this study, we focused a femtosecond laser (FL) on the skin of the hind leg muscles of living mice and investigated the clinical influence of the common acupuncture (ACP) on muscle disease via histological examination and expression analysis of the gene encoding myostatin [16]. In the histological examination, we observed damage of the skeletal muscle due to the femtosecond laser irradiation. We then used real-time PCR to estimate the gene expression and western blotting to estimate the protein translation of myostatin in the skeletal muscle after the laser irradiation. Myostatin is a growth repressor in muscle satellite cells [17]. The suppression of myostatin gene expression and protein translation indicates the facilitation of muscle cell proliferation. In comparison with the common acupuncture treatment, we recognized the potential of the femtosecond laser as a tool for the acupuncture.

2. Materials and methods

2.1. Laser stimuli

The experimental setup for the femtosecond laser (FL) is shown in Figure 1. Eight-week-old inbred strain C57BL/6 male mice were purchased from Japan SLC, Inc., Tokyo, Japan. After anesthesia treatment for the mice, hairs of the hind legs were saved and then mounted on an XY motorized stage (Sigma Koki, BIOS-215T). A femtosecond laser pulse train from a regeneratively amplified femtosecond laser system (Spectra Physics, Hurricane, 800 nm, 150 fs) was focused on the top of the hind leg through a quartz convex lens with a focus length of 150 mm. The laser irradiation was controlled by a mechanical shutter positioned in front of the laser system. The three-dimensional position of the laser focal spot was guided by a HeNe laser, with beams divided into two lines introduced on the focal spot from different directions. The laser focal spot was changed on the 1.5-cm-square area on the hind leg point to point with the XY motorized stage. The irradiation area was a little larger than the hind leg. The interval between the focal spots was set to 1 mm, and thus the laser irradiation was performed at 256 (16x16) points on the surface of the hind leg. Although the sample position fluctuated along the optical axis with a precision of a few millimeters, the focal spot size remained almost the same throughout the irradiation because the fluctuation is much smaller than the focus length of the focus lens (150 mm). By this manipulation, the laser irradiated almost the entire area of the hind leg. For each laser focal spot, a single- or 1000-shot laser pulse irradiated the target. For single-shot laser irradiation, a single-shot pulse was extracted from the pulse train at a repetition rate of 20 Hz by the mechanical shutter with a gate time of 50 ms. The 1000-shot laser pulse irradiation was performed by focusing the pulse

train at a rate of 1 kHz for 1 sec. The laser pulse energy was tuned to 300 mJ/pulse by a half-wave plate and polarizer.

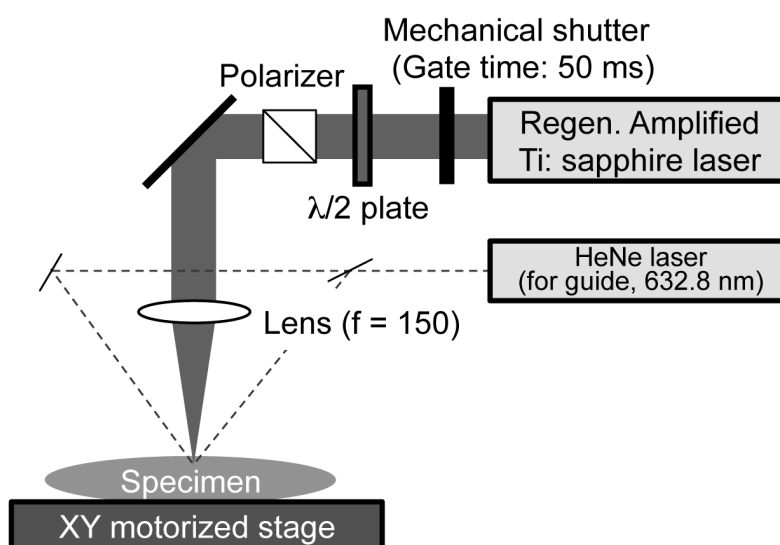


Figure 1. Experimental setup for femtosecond laser acupuncture.

After the laser stimulation, mice were treated for biological analyses to describe in the following sections. All mice in this research project were treated according to the Standards Relating to the Care and Management of Experimental Animals (Ministry of the Environment, Tokyo, Japan) [18]. This study was approved by the Committee for Safe Handling of Living Modified Organisms at Nara Institute of Science and Technology (permission number 1132) and Kobe University (permission number 17-21) and was carried out according to the guidelines of the committee.

2.2. Histochemical analysis

Tissue samples after the laser irradiation were fixed in 10% neutral buffered formalin and embedded in paraffin. Paraffin sections (3 mm thick) were stained with hematoxylin and eosin (H&E) as described previously [1,19].

2.3. Creatine kinase analysis

Blood samples were collected from mice after 3 hours of the laser irradiation. Creatine kinase (CK) assay was measured according to the manufacturer's instructions (L-Type CK kit, Wako Pure Chemical Industries, Japan) [20]. CK activity was determined by using a Hitachi autoanalyzer 7180 (Hitachi, Japan). The number of mice for each group in CK analysis was as follows: 9 for control, 11 for FL, 6 for ACP.

2.4. Real-time PCR analysis

To examine myostatin gene expression, total RNA was extracted from triceps surae muscle. Total RNA (5- μ g samples) was reverse-transcribed into cDNA by using SuperScript RT (SuperScript First-Strand Synthesis System; Life Technologies, Gaithersburg, MD), according to the company's instructions. Expression levels were compared by using real-time quantitative RT-PCR analysis with gene-specific primers as follows: myostatin: sense: 5'-GA-CAAAACACGAGGTACTCC-3'; antisense: 5'-GATTCAGCCCATCTTCTCC-3'. Real-time PCR was performed by using Power SYBR Green PCR Master Mix and StepOne (Applied Biosystems, Foster City, CA), according to the manufacturer's instructions. The reaction mixture consisted of 2 ml of SYBR Green, 4 ml of cDNA, and each primer at 5 pmol, plus water to a final volume of 20 ml. The PCR conditions were 95°C for 10 min followed by 50 cycles for 95°C for 15 s, 60°C for 60 s, and then 95°C for 15 s, 60°C for 60 s, and 95°C for 15 s. Internal control gene for this research was glyceraldehyde-3-phosphate dehydrogenase (GAPDH) [21,22]. The values of each group were expressed relative to those obtained for the control. The number of mice for each group in this analysis was as follows: 4 for control, 5 for FL, 6 for ACP.

2.5. Western blotting analysis

The triceps surae muscles were homogenized in PhosphoSafe reagent (Novagen, Madison, WI) supplemented with a protease inhibitor cocktail tablet (Roche, Indianapolis, IN). After centrifugation at 12,000 g for 25 min, the supernatant was frozen until use. Protein concentration was determined with Micro BCA Protein Assay Kit (Pierce, Rockford, IL) using bovine serum albumin as standard. For western blotting analysis, protein samples were resolved by SDS-PAGE and blotted on PVDF (Amersham, Piscataway, NJ). The primary antibodies used in this study were polyclonal anti myostatin antibody (Millipore, Billerica, MA) and α -tubulin loading control (Abcam, Cambridge, MA) [23]. The secondary antibody was a goat anti-rabbit IgG horseradish peroxidase (HRP) conjugate (Cell Signaling Technology, Danvers, MA). Immunoreactive bands were visualized with Pierce ECL Plus Western Blotting Substrate (Thermo Scientific, Rockford, IL) for α -tubulin, ECL Prime Western Blotting Detection System (GE Healthcare Life Sciences, Uppsala, Sweden) for myostatin. All blots were scanned, and the bands were analyzed with ImageJ software (<http://rsbweb.nih.gov/ij/>). The band densities were expressed relative to those obtained for the control. The number of mice for each group in this analysis was as follows: 5 for control, 6 for FL.

2.6. Statistical analysis

For CK and real-time PCR analyses, we used one-way ANOVA, followed by Tukey's post-hoc test. Data of western blotting were compared using unpaired Student's *t*-test. Data for and real-time PCR and western blotting were given as relative value to control with the data divided by the average value of control for normalization. The relative gene and protein levels of myostatin were calculated by means of comparison with the geometric mean of the translation of the internal control gene (GAPDH) and protein (α -tubulin), respectively. For all statistical analyses, maximum and minimum values are excluded from each group. All data

were presented as means \pm SD. *P* values of < 0.05 were considered statistically significant and the level of significance are expressed as follows in each figure: **, *P* < 0.01 ; ***, *P* < 0.001 ; NS, not significant.

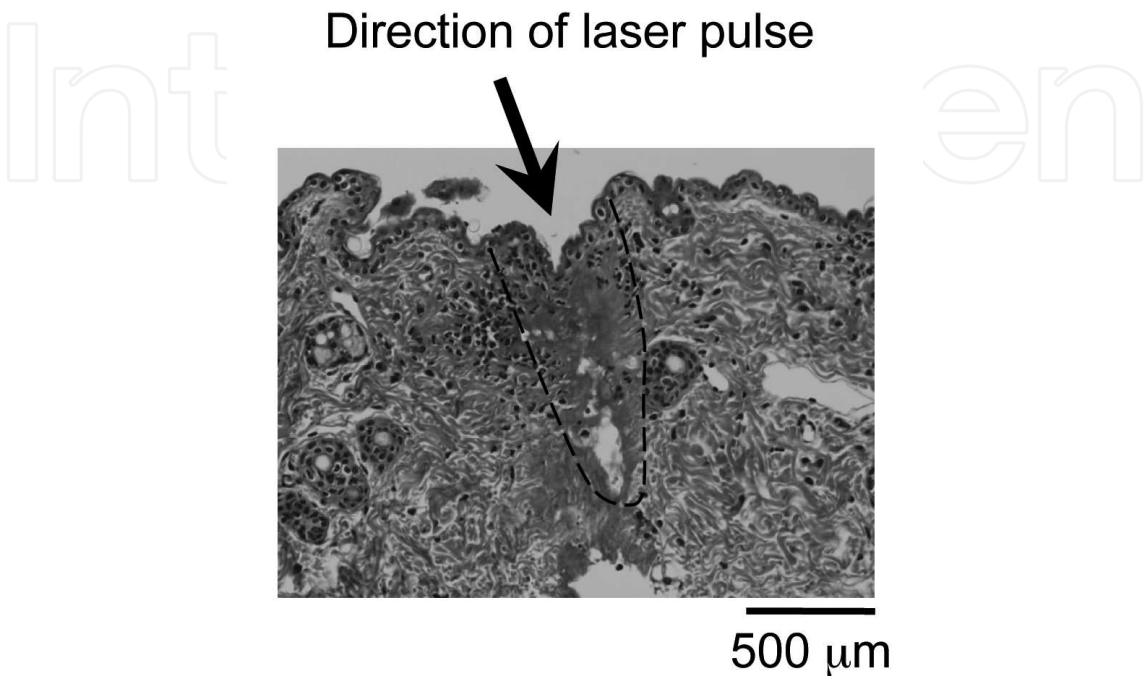


Figure 2. Histological microphotograph of the epidermis and dermis after single-shot irradiation with 300 uJ/pulse. The arrow indicates the direction of laser irradiation. The area within the dashed line was denatured by the laser irradiation. The skeletal muscle beneath the dermis was analyzed by real time-PCR and western blotting.

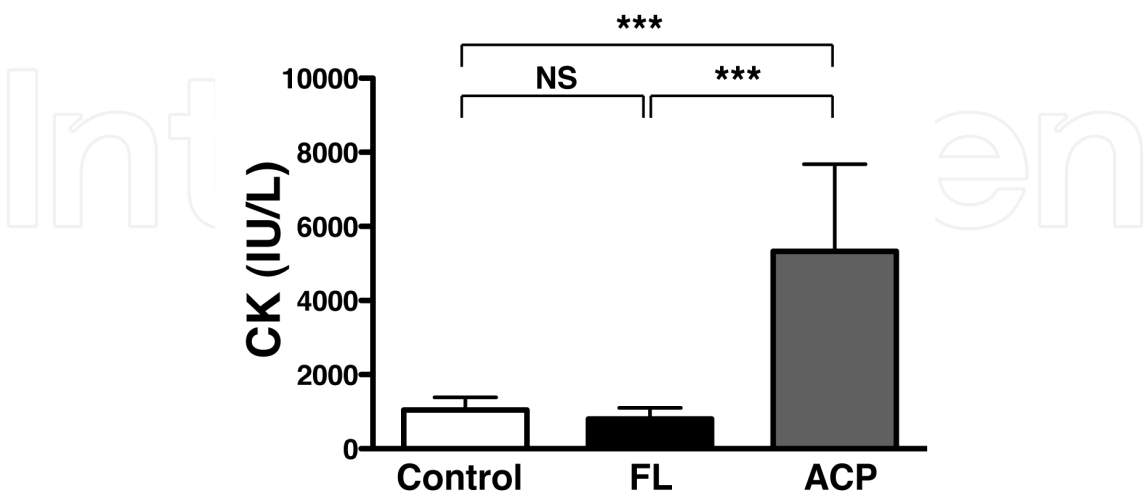


Figure 3. The serum creatine kinase after the femtosecond laser irradiation (FL) and common acupuncture stimuli (ACP).

3. Results and discussion

Figure 2b shows a representative histological microphotograph of epidermis and dermis with irradiation by a single-shot laser pulse with energy of 300 mJ/pulse. The microphotograph is a cross-section of a hind leg at a laser focal spot. The pulse energy was about 15 times larger than the ablation threshold (20 mJ/pulse). The diameter of the laser focal spot was about 30 μm , and we estimated the laser fluence and peak power density of the ablation threshold to be 0.7 J/cm² and 4.7×10^{12} W/cm², respectively. This is in rough agreement with the laser irradiation conditions reported as a threshold of the optical breakdown [8]. Under such conditions, the deposited laser energy is efficiently converted to shock and stress waves and propagates around the laser focal spot, as noted in the introduction. Along the axis of the laser irradiation and its surrounding area, the typical morphological pattern of the tissue was lost, indicating damage of the tissue. The diameter and depth of the damaged area were approximately 400 and 1100 μm , respectively (the area within the dashed line in (b)). Based on the depth, we estimated the absorption coefficient to be 10 cm⁻¹, which is reliable as an optical absorption property at 800 nm [9], though the absorption coefficient fluctuates greatly with the concentrations of melanin and hemoglobin. The diameter was larger than that of the laser focal spot size (about 30 μm), which means that the physical and/or physiological effects by the laser irradiation propagate from the area with the direct laser irradiation. Since a typical histological pattern due to heat denaturation was not observed in the damaged area, the damage was mainly induced by the photomechanical ablation. These results agree with those of previous studies [8,9]. Note that damage by the laser irradiation was not observed in the skeletal muscle (Figure 2a).

We evaluated the effects of laser on creatine kinase (CK) activity, because high level of CK means muscle damage [24]. Figure 3 indicates that the femtosecond laser irradiation (FL) dose not make injury in the muscle in contrast to ACP.

To reveal the muscle cell proliferation, the gene expression pattern of myostatin and GAPDH of the skeletal muscle after the laser irradiation was analyzed. The analysis was performed only for the skeletal muscle, from which epidermis and dermis were extracted. The expression of GAPDH, which is a kind of dehydrogenase, is not modulated by the environment surrounding changes in the tissue, the expression pattern was simultaneously monitored as an internal control of the gene expression of myostatin. Based on the ratio of the signal intensity of the pattern of myostatin to that of GAPDH, we can evaluate the gene expression of myostatin. Similarly, based on the ratio of the signal intensity of the pattern of myostatin to that of α -tubulin, we can evaluate the protein translation of myostatin because the translation of α -tubulin is stable in muscle.

Figure 4 shows the ratios after the femtosecond laser irradiation (FL) and common Acupuncture stimuli (ACP), which were normalized by the ratio of mouse hind leg muscle without laser irradiation (Control). An obvious suppression of myostatin gene expression was observed in case of laser irradiation and acupuncture. In addition, Figure 5 shows the myostatin translational ratios after the femtosecond laser irradiation (FL), which were normal-

ized by the ratio of mouse hind leg muscle without laser irradiation (Control). An obvious suppression of myostatin protein translation was observed in case of laser irradiation, too.

In the ACP treatment, skeletal muscles of the hind leg were directly stimulated by punctured. On the other hand, although the stimulation by the femtosecond laser irradiation was limited to the epidermis and dermis, as shown in Figure 2, suppression of the myostatin gene and protein were observed for the bulk of the skeletal muscle (Figures 4 and 5). As mentioned in the introduction, the photon energy absorbed by the tissue is considered to be effectively converted to energy to generate shock and stress waves [8-10]. This fact suggests that the skeletal muscle is stimulated by the propagation of shock and stress waves though the laser irradiation to the epidermis and dermis. This mechanical stimulation of the muscle facilitates muscle cell proliferation. Such shock and stress waves are generated by picosecond or nanosecond laser irradiation. However, because a great deal of photon energy is required for the generation in these cases, not only the epidermis and dermis but also skeletal muscle would have critical damage.

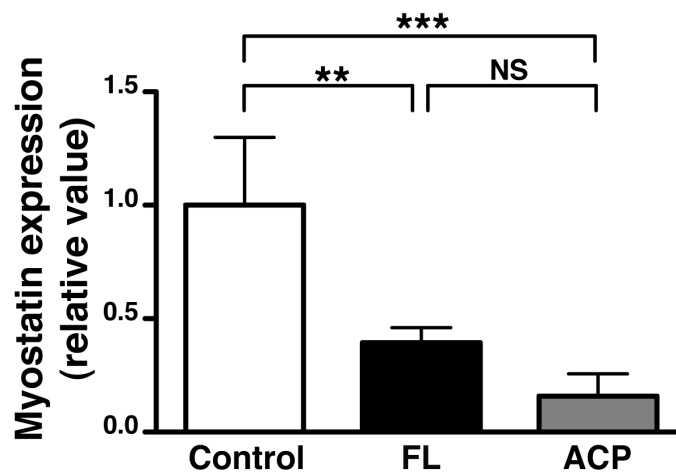


Figure 4. Real time-PCR analysis of myostatin gene expression after the femtosecond laser irradiation (FL) and common acupuncture stimuli (ACP). Relative transcript levels of myostatin were normalized with the signal intensity of the control. Glyceraldehyde-3-phosphate dehydrogenase (GAPDH) was used as an internal control.

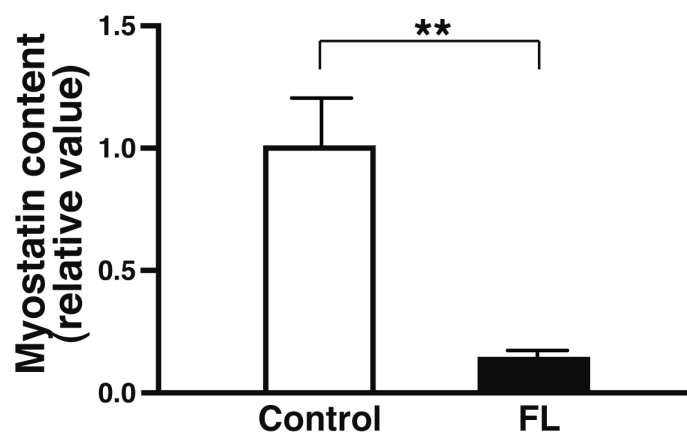


Figure 5. Western blotting analysis of myostatin translation under the femtosecond laser irradiation (FL) and common acupuncture (ACP). Relative protein levels of myostatin were normalized with the signal intensity of the control, and α -tubulin was used as an internal control.

4. Conclusion

Photomechanical ablation due to femtosecond laser irradiation was induced on hind leg muscles of living mice. Although the epidermis and dermis were denatured by the laser irradiation, a direct influence due to the laser irradiation was not observed in the skeletal muscle beneath the dermis. The gene expression of myostatin of the skeletal muscle after the laser irradiation was evaluated by real time-PCR and western blotting, and obvious suppression of the myostatin were identified in the bulk of hind leg muscle. The suppression, meaning the facilitation of muscle cell proliferation, was comparable to or greater than that of the skeletal muscle after EA treatment, which is a conventional acupuncture technique. On the basis of these results, we recognize the potential of the femtosecond laser as a tool for noncontact acupuncture for the treatment of muscle disease. Since our FL technique does not require the use of needles, such infection can be avoided. Furthermore, because it is possible to scan the skin with the laser beam using an electric optical device such as a Galvanomirror and acoustic-optical modulator, high-throughput, multipoint stimulation of muscle can be realized. We expect the present results will underscore the continuing potential of treatment by acupuncture.

Acknowledgements

We thank Mr. Kenji Miura for his technical assistance. This work was partly supported by a Grant-in-Aid for Scientific Research (C) (grant number 22590653) and (grant number 24590884) from the Japan Society for the Promotion of Science to Y.T. and M.O.; Grant-in-Aid for Scientific Research (Innovative Areas) (grant number 22120010) from the Japan Min-

istry of Education, Culture, Sports, Science and Technology (MEXT) to Y.H.; a Grant-in-Aid for Challenging Exploratory Research (grant number 22657041) from MEXT to Y.H.

Author details

Yutaka Takaoka^{1,2*}, Mika Ohta^{1,2}, Aki Sugano^{1,2}, Akihiko Ito³ and Yoichiro Hosokawa⁴

*Address all correspondence to: ytakaoka@med.kobe-u.ac.jp

1 Division of Medical Informatics and Bioinformatics, Kobe University Hospital, Chuo-ku, Kobe, Japan

2 Life Science Research Center, Kobe Tokiwa University, Nagata-ku, Kobe, Japan

3 Department of Pathology, Faculty of Medicine, Kinki University, Osaka-Sayama, Osaka, Japan

4 Graduate School of Materials Science, Nara Institute of Science and Technology (NAIST), Ikoma, Nara, Japan

References

- [1] Takaoka Y, Ohta M, Ito A, Takamatsu K, Sugano A, Funakoshi K, Takaoka N, Sato N, Yokozaki H, Arizono N, Goto S, Maeda E. Electroacupuncture suppresses myostatin gene expression: cell proliferative reaction in mouse skeletal muscle. *Physiol Genomics* 2007; 30: 102-110.
- [2] Ohta M, Sugano A, Goto S, Yusoff S, Hirota Y, Funakoshi K, Miura K, Maeda E, Takaoka N, Sato N, Ishizuka H, Arizono N, Nishio H, Takaoka Y. Full-length sequence of mouse acupuncture-induced 1-L (aig1l) gene including its transcriptional start site. *Evid Based Complement Alternat Med* 2009; 2011: 249280.
- [3] Ikemune S, Ohta M, Suzuki S, Machida M, Takemasa T, Takaoka Y, Miyamoto T. Electroacupuncture accelerates recovery of muscle atrophy induced by hindlimb suspension in mouse skeletal muscle (in Japanese). *Journal of the Japan Society of Acupuncture and Moxibustion* 2010; 60(4): 707-715.
- [4] Ikemune S, Ohta M, Miyamoto T, Takaoka Y. Molecular Mechanisms of Inhibiting the Muscle Atrophy by Electroacupuncture (in Japanese). *The Journal of the Japanese Society of Balneology, Climatology and Physical Medicine* 2011; 74(2): 103-111.
- [5] Zhang X. Acupuncture: Review and Analysis of Reports on Controlled Clinical Trials. <http://apps.who.int/medicinedocs/en/d/Js4926e/> (accessed 12 August 2012)

- [6] Culliton BJ. NIH says “yes” to acupuncture. *Nat Med* 1997; 3: 1307.
- [7] Klein JL, Trachtenberg IA. Acupuncture. *Current Bibliographies in Medicine* 97-6 <http://www.nlm.nih.gov/pubs/cbm/acupuncture.html> (accessed 12 August 2012)
- [8] Vogel A, Noack J, Hüttman G, Paltauf G. Mechanisms of femtosecond laser nanosurgery of cells and tissues. *Applied physics B* 2005; 81(8): 1015-1047.
- [9] Vogel A, Venugopalan V. Mechanisms of pulsed laser ablation of biological tissues. *Chem Rev* 2003; 103(2): 577-644.
- [10] Hosokawa Y, Yashiro M, Asahi T, Masuhara H. Photothermal conversion dynamics in femtosecond and picosecond discrete laser etching of Cu-phthalocyanine amorphous film analysed by ultrafast UV–VIS absorption spectroscopy. *Journal of Photochemistry and Photobiology A: Chemistry* 2001; 142: 197-207.
- [11] Hosokawa Y, Takabayashi H, Miura S, Shukunami C, Hiraki Y, Masuhara H. Non-destructive isolation of single cultured animal cells by femtosecond laser-induced shockwave. *Applied physics A* 2004; 79(4-6): 795-798.
- [12] Kaji T, Ito S, Miyasaka H, Hosokawa Y, Masuhara H, Shukunami C, Hiraki Y. Non-destructive micropatterning of living animal cells using focused femtosecond laser-induced impulsive force. *Applied Physics Letters* 2007; 91: 023904.
- [13] Kuo Y, Wu C, Hosokawa Y, Maezawa Y, Okano K, Masuhara H, Kao F. Local stimulation of cultured myocyte cells by femtosecond laser-induced stress wave. *Applied Physics A* 2010; 101(4): 597-600.
- [14] Hagiyaama M, Furuno T, Hosokawa Y, Iino T, Ito T, Inoue T, Nakanishi M, Murakami Y, Ito A. Enhanced nerve-mast cell interaction by a neuronal short isoform of cell adhesion molecule-1. *J Immunol* 2011; 186(10): 5983-5992.
- [15] Hosokawa Y, Hagiyaama M, Iino T, Murakami Y, Ito A. Non-contact estimation of intercellular breaking force using a femtosecond laser impulse quantified by atomic force microscopy. *Proceedings of the National Academy of Sciences* 2011; 108: 1777-1782.
- [16] Carlson CJ, Booth FW, Gordon SE. Skeletal muscle myostatin mRNA expression is fiber-type specific and increases during hindlimb unloading. *Am J Physiol* 1999; 277(2 Pt 2): R601-606.
- [17] Trendelenburg AU, Meyer A, Rohner D, Boyle J, Hatakeyama S, Glass DJ. Myostatin reduces Akt/TORC1/p70S6K signaling, inhibiting myoblast differentiation and myotube size. *Am J Physiol Cell Physiol* 2009; 296(6): C1258-1270.
- [18] Ministry of the Environment T, Japan. Standards Relating to the Care and Management, etc. of Experimental Animals. http://www.env.go.jp/nature/dobutsu/aigo/2_data/nt_h180428_88.html (accessed 12 August 2012)

- [19] Takaoka Y, Ohta M, Miyakawa K, Nakamura O, Suzuki M, Takahashi K, Yamamura K, Sakaki Y. Cysteine 10 is a key residue in amyloidogenesis of human transthyretin Val30Met. *Am J Pathol* 2004; 164: 337-345.
- [20] Morin LG. Creatine kinase: re-examination of optimum reaction conditions. *Clin Chem* 1977; 23(9): 1569-1575.
- [21] Barber RD, Harmer DW, Coleman RA, Clark BJ. GAPDH as a housekeeping gene: analysis of GAPDH mRNA expression in a panel of 72 human tissues. *Physiol Genomics* 2005; 21: 389-395.
- [22] Jemiolo B, Trappe S. Single muscle fiber gene expression in human skeletal muscle: validation of internal control with exercise. *Biochem Biophys Res Commun* 2004; 320: 1043-1050.
- [23] Ochi E, Hirose T, Hiranuma K, Min SK, Ishii N, Nakazato K. Elevation of myostatin and FOXOs in prolonged muscular impairment induced by eccentric contractions in rat medial gastrocnemius muscle. *J Appl Physiol* 2010; 108(2): 306-313.
- [24] Brancaccio P, Lippi G, Maffulli N. Biochemical markers of muscular damage. *Clin Chem Lab Med* 2010; 48(6): 757-767.

IntechOpen

